Iran University of Science and Technology

**International Journal of Automotive Engineering**

**Journal Homepage: ijae.iust.ac.ir**

ISSN: 2008-

# Antilock Regenerative Braking System Design for a Hybrid Electric Vehicle

**M. Esfahanian[1*], M.Saadat[2], P. karami[2]**

[1,3]Department of Mechanical Engineering, Isfahan University of Technology, Isfahan, 8415683111, Iran

[2]Department of Mechanical Engineering, Faculty of Engineering, Najafabad Branch, Islamic Azad University, Najafabad, Isfahan, Iran.

**ARTICLE INFO**

**Article history**:
Received : 02-Dec-2017
Accepted: 04-Jul-2018
Published:

**Keywords**:
Antilock braking system
Antilock hydraulic braking
Fuzzy controller
Regenerative braking

**A B S T R A C T**

Hybrid electric vehicles employ a hydraulic braking system and a regenerative braking system together to provide enhanced braking performance and energy regeneration. In this paper an integrated braking system is proposed for an electric hybrid vehicle that include a hydraulic braking system and a regenerative braking system which is functionally connected to an electric traction motor. In the proposed system, four independent anti-lock fuzzy controllers are developed to adjust the hydraulic braking torque in front and rear wheels. Also, an antiskid controller is applied to adjust the regenerative braking torque dynamically. A supervisory controller, is responsible for the management of this system. The proposed integrated braking system is simulated in different driving cycles. Fuzzy rules and membership functions are optimized considering the objective functions as SoC and slip coefficient in various road conditions. This paper considers different issues in design process such as the antilock performance of the regenerative braking system, non-interference performance of the regenerative and hydraulic braking system on the front axle, maximum torque of the electric motor, SoC monitoring, calculating the velocity for four wheels and the roads with different slip and cornering conditions. The simulation results show that the fuel consumption and the energy loss in the braking is reduced. In the other hand, this energy is regenerated and stored in the batteries, especially in the urban cycles with high start/stop frequency. The slip ratio remains close to the desired value and the slip will not occur in the whole driving cycle. Therefore, the proposed integrated braking system can be considered as a safe, anti-lock and regenerative braking system.

## 1. Introduction

Environmental concerns and diminishing fossil fuel resources, has forced the automakers to move toward reducing fuel consumption. As of today, the hybrid electric vehicle is the best choice that can satisfy this demand. Hybrid electric vehicles (HEVs) have multiple power sources for vehicle propulsion which provide great ease and flexibility to achieve advanced controllability and better driving performance. One of the most important features of HEVs is their ability to regenerate significant amount of braking energy.

*Corresponding Author
Email Address:
mesf1964@cc.iut.ac.ir

Anti-lock brake control systems for a conventional vehicle based on fuzzy inference systems are presented in the previous studies. However, the control systems presented in those papers were aimed to be applied only in the conventional vehicles in which the regenerative braking is not considered in the control system. In the other hand, an intelligent control strategy is needed to provide an antiskid braking system for hybrid electric vehicles that improves braking performance. This strategy should achieve maximum regenerative braking energy and minimum kinetic energy loss and also should coordinate hydraulic and regenerative braking torque together. The recent research on hybrid electric vehicles is focused on efficiency improvement and emission reduction with the constraint of safe braking without locking the wheels, which can be accomplished by a combined control strategy of the regenerative and anti-lock braking system.

Brake control system design using iterative learning control is studied in 2005 [1]. A novel regenerative braking algorithm was proposed based on regenerative torque optimization with emulate engine compression braking [2]. A regenerative braking was designed for a hybrid bus with a neuro-fuzzy algorithm that is established through combination of the fuzzy algorithm and the back-propagation (BP) networks [3]. A combined braking control strategy for regenerative and hydraulic brake systems is also presented [4]. A novel hybrid antiskid braking system using fuzzy logic is proposed for a hybrid electric vehicle in which a regenerative braking system was associated to an electric traction motor and the vehicle has a separate hydraulic braking system [5]. An adaptive rule based controller for an anti-lock regenerative braking system (ARBS) of a series hybrid electric bus (SHEB) has been proposed [6]. The proposed controller integrates the regenerative braking and wheel antilock functions by controlling the electric motor of the hybrid vehicle, without using any conventional mechanical antilock braking system. A method was proposes to recover more energy in the process of braking for hybrid electric vehicle using rear motor control [7]. A fuzzy control strategy is designed to determine the distribution between hydraulic braking force and regenerative braking force for the rear wheels braking force. An anti-lock regenerative braking strategy is proposed to attain anti-slip control for negative accelerations [8]. A regenerative brake patched on ABS module in a hybrid vehicle is considered [9]. To optimize the output voltage accumulated in the battery the nominal value of some important elements like capacitor, inductor and initial power of battery, are considered by an evolutionary algorithm based on genetic algorithms. According to the variation of the adhesion coefficient under different roads, the maximum adhesion force and the optimal slip ratio are calculated in real-time [10]. An intelligent tire system is utilized to detect varying road surfaces to obtain friction information and optimal operation slip ratio. In addition, the HEV eight- degree- of- freedom dynamics model is developed for ABS control, which includes the LuGre tire model [11]. In order to improve energy utilization rate of battery-powered electric vehicle (EV) using brushless DC machine (BLDCM), the model of braking current generated by regenerative braking and control method are discussed [12].

Unfortunately, some important factors such as the battery's SoC, anti-skid braking performance of the regenerative braking system, synchronize performance of the hydraulic and regenerative braking systems are not considered in the reviewed papers. In this paper an integrated braking system is proposed that include a hydraulic braking system and a regenerative braking system which is functionally connected to an electric traction motor. In the proposed system, four independent anti-lock fuzzy controllers are developed to adjust the hydraulic braking torque in front and rear wheels. Also, an antiskid controller is applied to adjust the regenerative braking torque dynamically. A supervisory controller, is responsible for the management of this system. The proposed integrated braking system is simulated in different driving cycles. Fuzzy rules and membership functions are optimized considering the objective functions as SoC and slip coefficient in various road conditions.

The proposed integrated braking system design is presented in section 2 including brake control algorithm and the fuzzy logic. The proposed integrated braking system is simulated in different driving cycles in section 3. The results are discussed in section 4.

## 2. Integrated braking system design

A schematic diagram of an integrated braking system is shown in Figure 1.

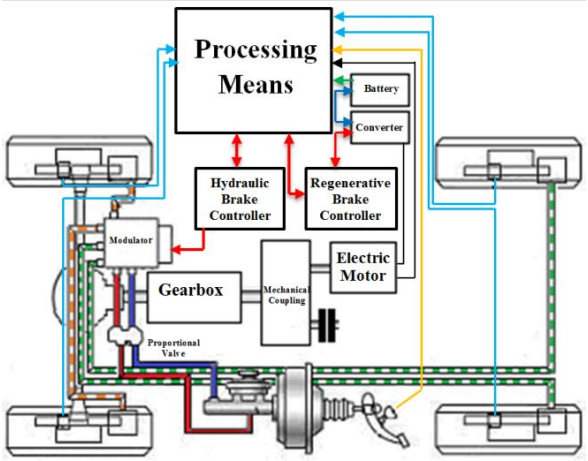


**Figure 1:** Schematic diagram of an integrated braking system [13].

This braking system in a hybrid electric vehicle includes a regenerative braking system which is functionally connected to an electric traction motor in the front axle and a separate hydraulic braking system which is connected to all wheels. The mentioned braking system have some sensors for monitoring vehicle parameters and a processor for calculating the vehicle state based on the sensors data. The vehicle state is not directly measurable by the sensors and it can be used to determine that the regenerative anti-skid braking system requires the hydraulic braking to be activated or not. The processor employs a fuzzy logic controller based on the determined vehicle state and provides appropriate command signals to the motor controller. In addition, command signals are send to the brake controller to adjust the applied fluid pressure at each wheel to provide appropriate regenerative and hydraulic brake.

### 2.1. Brake control algorithm

Figure 2 shows a flow chart illustrating the proposed strategy for the regenerative anti-skid braking according to the designed braking system.

1) Upon starting the vehicle, predetermined values are assigned to the system variables initially. Vehicle parameter are then sensed through the sensing elements and then central processor receives required input signals. This input signals include: individual speed of each wheel, hydraulic brake pressure to driven wheels, electric motor speed and the pedal position.
2) Additional vehicle parameters (which are not directly measurable by mentioned sensing elements) are calculated by the processing mean. This parameters include: the slip $\lambda_d$, adhesion coefficient $\mu_d$, vehicle speed $v$, vehicle acceleration $D_v$ and the other effective parameters corresponding to Equations (4) to (9). In the following equations, the subscript zero indicates the parameter values associated with previous time fraction and subscript $d$ describes the drive shaft parameters.

$$\lambda_d = (\omega_d - (v/R_w))/(v/R_w) \quad (1)$$

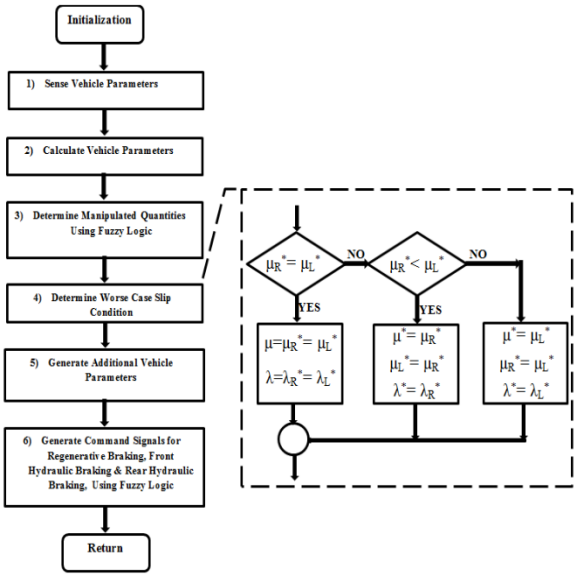


**Figure 1:** Flow chart of the integrated braking control algorithm [13].

$$\mu_d = [K(2(\theta_e/G_r) - \theta_{Rd} - \theta_{Ld}) + B(2(\omega_e/G_r) - \omega_{Rd} - \omega_{Ld}) - 2\tau_d - 2J_r\alpha_d]/(2R_w N_v) \quad (2)$$

$$N_v = ((W \times C)/2L) - ((W \times D_v \times h)/2gL \quad (3)$$

$$\Delta\mu_d = \mu_d - \mu_{d0} \quad (4)$$

$$\Delta\lambda_d = \lambda_d - \lambda_{d0} \quad (5)$$

$$s_{1d} = \mu_d/\mu_{d0} \quad (6)$$

$$s_{2d} = \Delta\mu_d/\Delta\lambda_d \quad (7)$$

$$s_{3d} = s_{2d}/s_{2d0} \quad (8)$$

$$\Delta\lambda_d^* = \lambda_d - \lambda_{d0}^* \quad (9)$$

In a state requiring braking control, wheel slip for each driven wheel $\lambda_d$ is calculated according to the Equation (1), wherein $\omega_d$ is the wheel speed of subject driven wheel and v is vehicle speed and $R_w$ is the wheel radius [13]. Also in Equation (2), $K$ is the spring rate of the vehicle drive axle, $\theta_e$ is the speed integral of the electric motor, $G$ is the combined gear ratio of the differential and the transmission, $\theta_{rd}$ and $\theta_{ld}$ are the speed integrals of the right and left driven wheels respectively, $J_r$ is the wheel inertia, $B$ is the damping rate between the motor shaft and the wheels due to the bearings, $\omega_e$ is the electric motor speed, $\omega_{rd}$ and $\omega_{ld}$ are the right and left driven wheel speeds, $\alpha_{rd}$ and $\alpha_{ld}$ are acceleration rates of the right and left driven wheels, $\tau_d$ is the hydraulic brake torque applied to the monitored driven wheel, $N_v$ is the normal force on the respective wheel. In Equation (3), $W$ is the vehicle weight, $C$ is the distance between the vehicle center of gravity and the center of rear axle, $L$ is the center of gravity's height from road surface and $g$ is the acceleration of gravity at the earth surface.

3) The calculated parameters in step 2 are the input parameters for step 3. The processing unit then determines various manipulated quantities using fuzzy logic. This quantities include critical adhesion coefficient $\mu^*$ and critical wheel slip $\lambda^*$ for each driven wheel.
4) After determining the corresponding critical adhesion coefficient and critical wheel slip for each driven wheel, the processing unit next determines the worst case slip condition (Figure 2). Outputs of this step are used as the slip threshold conditions for regenerative brake in step 6. In fact, when the worst case slip are used as the slip threshold conditions of the regenerative brake system, the functional interactions of the regenerative and hydraulic brake systems will not occur.
5) In this step, additional vehicle parameters are calculated. These parameters include: $\tau_{Fmax2}$ the maximum brake torque that can be applied to the front wheels just before the skid point (with no braking torque applied to the rear wheels), $\tau_{Fmax4}$ the maximum brake torque that can be applied to the front wheels just before skid where brake torque is applied to all four wheels and $\tau_{Rmax}$ the maximum brake torque that can be applied to the rear wheels just before skid when brake torque is applied to all four wheels. These parameters can be calculated according to the following equations:

$$\tau_{F\max 2} = R_w[(\mu^* N_v C)/(L - \mu^* h)] \quad (10)$$

$$\tau_{F\max 4} = R_w[(\mu^* N_v)/L] \times (C + \mu^* h) \quad (11)$$

$$\tau_{R\max} = R_w[(\mu^* N_v)/L] \times (B - \mu^* h) \quad (12)$$

Wherein $C$ is the distance between the center of gravity and the rear axle center, $h$ is the of the center of gravity's height, $L$ is the wheel base and $B$ is the distance between center of the gravity and the front axle center. In addition, $s_1$ to $s_{11}$ are calculated according to the following equations and are used as the inputs for the fuzzy controller in step 6.

| | |
|---|---|
| $s_4 = \tau_d - \tau_{regavailable}$ | (13) |
| $s_5 = \tau_{F\max 2} - \tau_d$ | (14) |
| $s_6 = \tau_{regavailable} - \tau_{F\max 4}$ | (15) |
| $s_7 = \tau_d - \tau_{regavailable} - \tau_{R\max}$ | (16) |
| $s_8 = \tau_{F\max 4} - \tau_{regdemand}$ | (17) |

| | |
|---|---|
| $s_9 = \tau_d - \tau_{regdemand}$ | (18) |
| $s_{10} = \tau_d - \tau_{F\max 4} - \tau_{R\max}$ | (19) |
| $s_{11} = \tau_d - \tau_{F\max 4}$ | (20) |

Wherein $\tau_d$ is the torque demanded by the driver, $\tau_{regavailable}$ is the available regenerative brake torque and $\tau_{regdemand}$ is the regenerative brake torque demanded. The brake torque is proportional to the hydraulic fluid pressure.

6) Fuzzy logic is applied to the sensed and calculated vehicle parameters by the processing unit to generate the command signals for the regenerative braking, front hydraulic braking and rear hydraulic braking.

### 2.2 Fuzzy Logic

Figure 3 is a graphical representation of the inter-relationship of $\mu$ the adhesion coefficient between wheel and road surface and $\lambda$ the wheel slip or skid. Quadrant III in this figure illustrates the conditions corresponding to regenerative antiskid braking control. Quadrant I illustrates conditions corresponding to traction control. According to the curve drawn in quadrant I of Figure 3, the adhesion coefficient $\mu$ will increase by increasing the wheel slip $\lambda$ until a critical value of $\lambda^*$ denoted by the vertical line. As wheel slip $\lambda$ increases beyond the critical slip value, the wheel enters the free spin region. Also, as illustrated by the curve drawn in quadrant III in Figure 3, the adhesion coefficient $\mu$ decrease as wheel slip $\lambda$ decrease until a critical value of wheel slip $\lambda^*$, denoted by a vertical line. Beyond this critical skid value, the adhesion coefficient $\mu$ increases and the wheel approaches lock-up, which leads to vehicle instability. Therefore, it is necessary to determine the critical values of slip and adhesion coefficient for regenerative braking control. In step 3, the processing unit determines critical adhesion coefficient $\mu^*$ and critical wheel slip $\lambda^*$ for each driven wheel using fuzzy logic. Fuzzy membership functions and rule bases associated with these fuzzy controllers has been shown in Figure 4 and Figure 5.

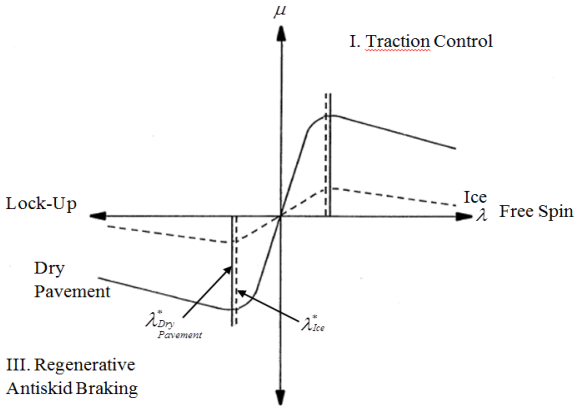


**Figure 3:** Graphical representation of adhesion and slip coefficients at different road surfaces.

According to the Figure 3, general logics (G.L.1-4) of the rules in Figure 4 can be described as:

G.L.1: When the slip coefficient is greater than its critical value in previous moment, with increase of slip and adhesion coefficient, the amount of critical slip coefficient and the adhesion related with those will increase.

G.L.2: When the slip coefficient is greater than critical slip coefficient value in previous moment, with decrease of slip and adhesion coefficient, the amount of critical slip coefficient and the adhesion related with those will increase.

G.L.3: According to the Figure 3, with increase in the slip coefficient, decrease in adhesion coefficient and larger increase in the difference of it with adhesion coefficient value in previous moment and larger increase in the slope of the chart, the amount of critical slip coefficient and the adhesion related with those will increase.

G.L.4: According to the Figure 3, with decrease of the slip coefficient, decrease in adhesion coefficient and larger increase in the difference of it with adhesion coefficient value in previous moment and larger increase in the slope of the chart, the amount of critical slip coefficient and the adhesion related with those will increase.

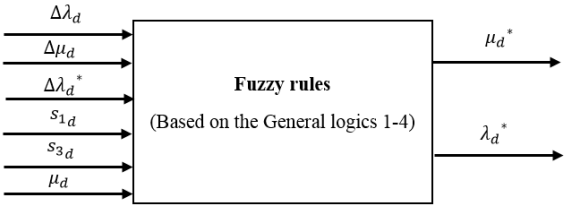


**Figure 4:** Fuzzy system used to determine critical wheel slip λ*d and critical adhesion coefficient μ*d.

Wheel slid $\lambda$ is always negative when regenerative anti-skid braking control is required because of the tension caused by the braking demand. As illustrate by the curve drawn in quadrant III, in Figure 3, the adhesion coefficient $\mu$ decrease as wheel slip $\lambda$ decrease until a critical value of wheel slip $\lambda$*, denoted by vertical line. Beyond this critical skid value, the adhesion coefficient $\mu$ increases and the wheel approaches lock-up, which leads to vehicle instability. To regain vehicle stability when a condition of excessive skid exists, regenerative motor braking torque must be reduced so the driven wheels can accelerate to speed that allows for the maximum traction between the tire and road surface. Optimal vehicle deceleration occurs when the wheel skid $\lambda$ is at the critical wheel skid $\lambda^*$ for the present road surface. This is a general principle in the design of the fuzzy controller for regenerative and hydraulic braking systems. Also, for prevention of regenerative and hydraulic brake system functional interactions on the front axle and provide sufficient braking power on the rear wheels, general principles (G.P. 1-8) are considered.

G.p.1: When the torque demanded by the driver $\tau_d$, is smaller than the available regenerative brake torque $\tau_{regavailable}$, and the amounts of the slip and adhesion coefficient are smaller than the critical values, all of the required braking torque will be provided by the regenerative braking system.

G.P.2: When the regenerative braking system can provided all of the torque demanded by driver $\tau_d$, and the amounts of the slip and adhesion coefficient are smaller than the critical values, with increase of the required braking torque, the regenerative braking torque is increased.

G.P.3: $\tau_{Fmax2}$, $\tau_{Fmax4}$ and $\tau_{Rmax}$ are effective and limiting parameters for determine the applied braking torque on each wheels. Therefore, whatever the required braking torque is greater than $\tau_{Fmax2}$, then the amount of the applied braking torque on each wheels decrease.

G.P.4: With larger increase in the difference of $\tau_{Fmax4}$ with available regenerative brake torque $\tau_{regavailable}$, the amount of the regenerative braking torque is decreased and the amount of the hydraulic braking torque applied on the front wheels is increased.

G.P.5: Whatever the amount of the required braking torque $\tau_d$, is smaller than the total of the available regenerative brake torque $\tau_{regavailable}$ and $\tau_{Rmax}$, the amount of the hydraulic braking torque applied on the front and rear wheels is decreased.

G.P.6: Whenever the amount of the $\tau_{Fmax4}$ is greater than the amount of the available regenerative brake torque $\tau_{regavailable}$, the amount of the hydraulic braking torque applied on the front wheels is increased.

G.P.7: Whatever the amount of the required braking torque $\tau_d$, is greater than the regenerative brake torque demanded $\tau_{regdemand}$, the amount of the hydraulic braking torque applied on the rear wheels is increased.

G.P.8: Whenever the amount of the required braking torque $\tau_d$, is greater than the amount of the $\tau_{Fmax4}$ and also the total of the $\tau_{Fmax4}$ and $\tau_{Rmax}$, the amount of the hydraulic braking torque applied on the rear wheels is increased.

In Figures 5 to 7, the fuzzy controllers used in step 6 has been shown.

## 3. Analysis and Simulation

Designed integrated braking system is modeled in MATLAB/ADVISOR [15]. Thus, the dynamic model of the vehicle and its components are similar to the model used in software ADVISOR, a 5 DOF (Degrees-of-Freedom) non-linear vehicle model with non-steady semi-empirical tire model,

an experimental motor-battery model. In the control blocks of ADVISOR, the required primary inputs in step 1, include electric motor speed, braking pedal position and the amount of the required braking torque are available. ADVISOR can't provide the speed of the wheels separately. Therefore, in this modeling, semi-empirical model using in the ADVISOR are applied for each wheel. Speed of the wheels calculated by Equation (9) separately and required slip coefficient is obtained from Table 1.

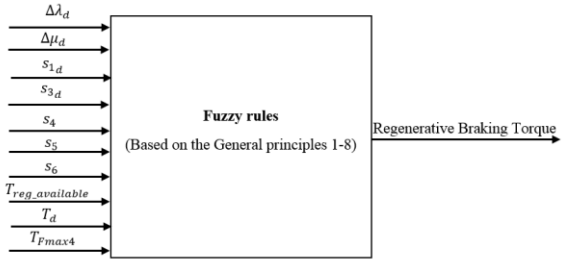


**Figure 5:** Fuzzy system used to determine regenerative braking torque.

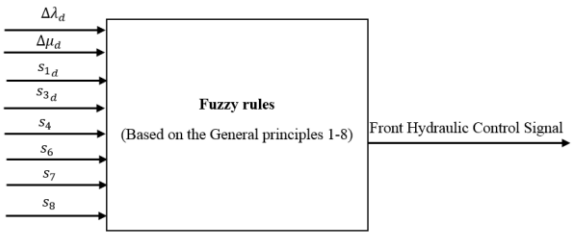


**Figure 6:** Fuzzy system used to determine regenerative braking torque.

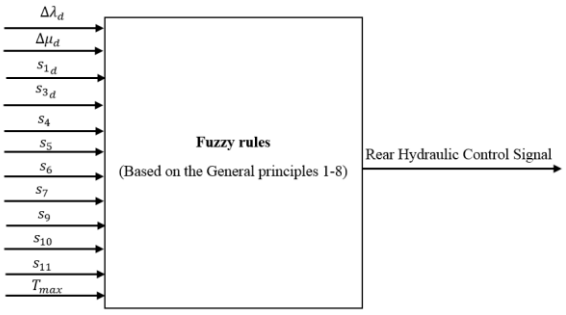


**Figure 7:** Fuzzy system used to determine regenerative braking torque.

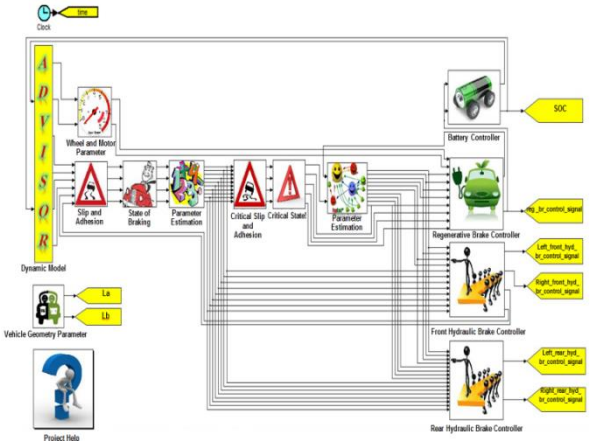


**Figure 8:** Designed integrated braking system.

**Table 1. Slip coefficient [14]**

| $(\frac{F_x}{F_z})$ | $\lambda_{dLeft}$ | $\lambda_{dRight}$ |
|---|---|---|
| 0 | 0 | 0 |
| 0.025 | 0.3913 | 0.25 |
| 0.050 | 0.6715 | 0.50 |
| 0.075 | 0.8540 | 0.75 |
| 0.100 | 0.9616 | 0.10 |
| 0.125 | 1.0212 | 0.125 |

Coefficient and parameters used in this simulation are shown in Table 2.

**Table 2. Effective parameter in simulation**

| | |
|---|---|
| Vehicle weight | 1278 [kg] |
| Wheel inertia | 3.2639 [$Kg\,m^2$] |
| Wheel radius | 0.282 [m] |
| Wheelbase | 2.4 [m] |
| Wheel tread front/rear | 1.7368 [m] |
| Max. of engine power | 41 [kW] |

In simulation, velocity and acceleration of vehicle is available by driving cycle and the other control parameters calculated according to the

Equation (1)-(9). In step 3, the critical slip conditions are determined by fuzzy logic controllers. Then, worst critical slip condition are determined and the other required parameters are calculated. At the end, fuzzy logic controllers calculated the regenerative and hydraulic braking torque.

Considering Figures 5-7, the membership functions are in the specific numerical ranges (-1, 1), and the gain coefficients are needed. Simulated control system run in nine standard driving cycles. Gain coefficient of each cycle has been determined and the smallest of the coefficients is selected. Also, simulated control system run in the combined cycle and gain coefficients has been calculated.

Simulated control system run in NEDC and TEHRAN cycles and its performance in terms of safety, stability and waste energy recovery has been investigated. In Figures 9-11, performance of the simulated braking system in NEDC cycle has been shown.

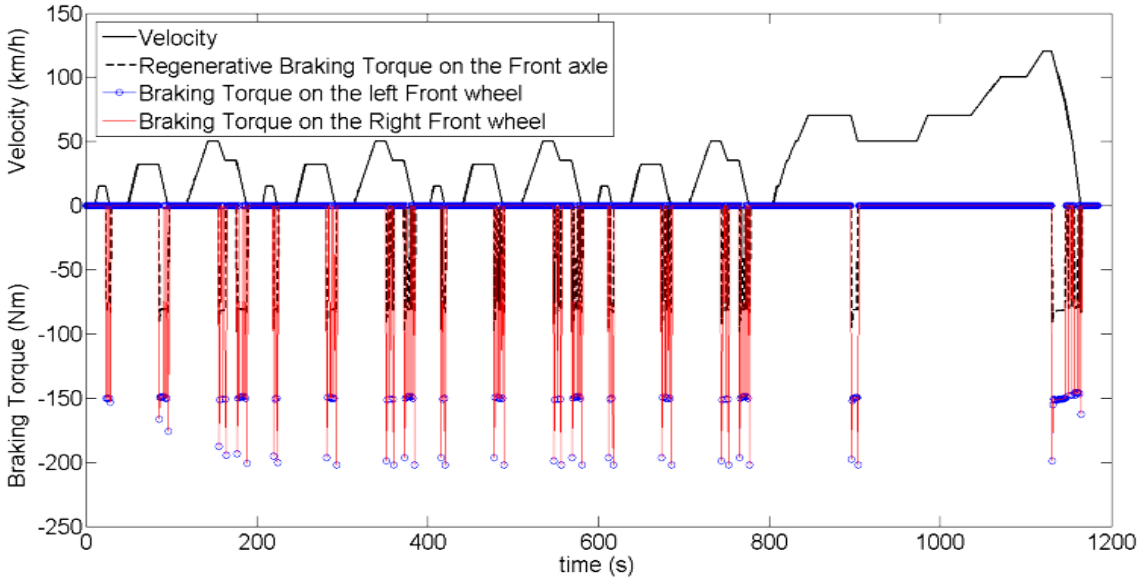


**Figure 9. Braking torque on the front axle, NEDC cycle.**

The simulation results of a research in 2008 [14] are shown in Figure 12. As illustrated, in the braking process, the electric motor acts as the main braking source, and the hydraulic braking system works only to ensure the parking. In this simulation high power electric motor has been use, therefore the possibility of providing the required braking torque has been created. The performance of the controller in some of the cycle times, especially in the ECE cycle is weak. Also, the anti-lock performance of the system is not visible.

In Figure 13 regenerative braking torque in integrated braking system, compared with regenerative braking torque from reference [14] are illustrated. The amount of the regenerative braking torque in integrated braking system, with the anti-lock characteristics, is smaller than the amount of the regenerative braking torque from reference. Of course, the slip condition and performance of electric motors for the two simulations are different. The remaining amount of the required braking torque by the hydraulic brake system will be provided, but sum of the regenerative and hydraulic braking torques is equal to the required braking torque.

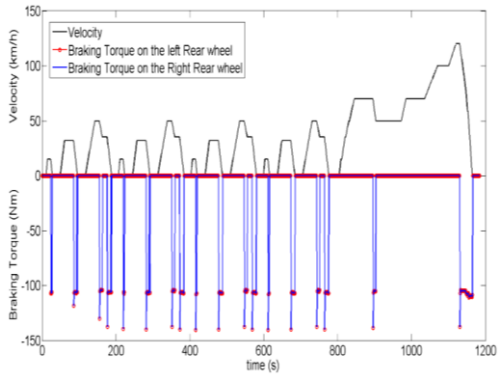


Figure 10:Braking torque on the rear axle, NEDC cycle.

In Figures 14-16, performance of the simulated braking system in Tehran driving cycle [16] has been shown. In this cycle, a distance of 13.42 km with an average speed of 26.88 km/h and a maximum speed of 83.94 km/h in the 1797 s, is traveled.

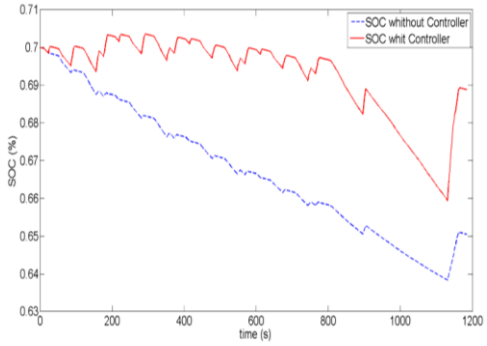


**Figure 11**: Battery SoC, NEDC cycle

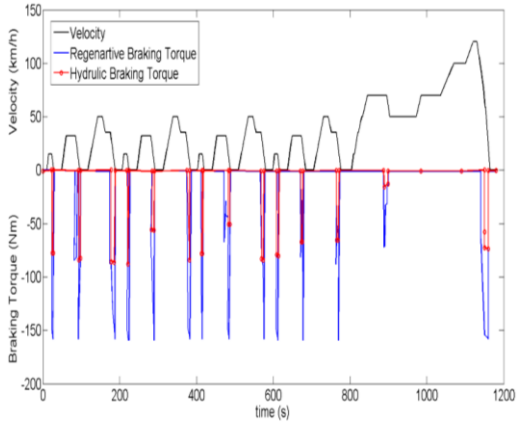


**Figure 12**. Braking torque on the front axle, NEDC cycle [14]

According to the obtained results, the anti-lock performance of the regenerative braking system and hydraulic braking system, sufficient brake power provided by these two systems; non-interference performance of those can be seen.

According to the Fig.17, at the end of the driving cycle, the battery SoC is increased from 0.64 to 0.75, is the result of the high frequent stop-and-go traffic.

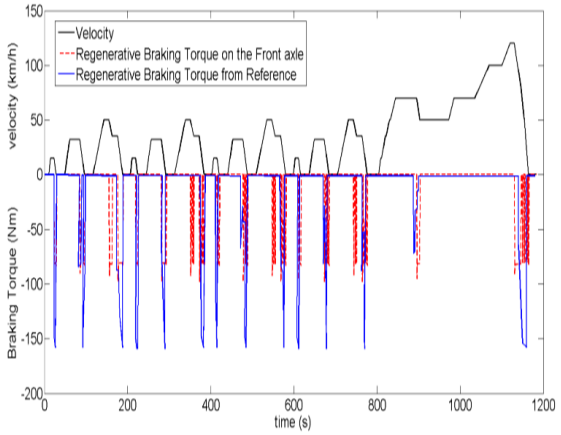


**Figure 13.** Regenerative braking torque, NEDC cycle

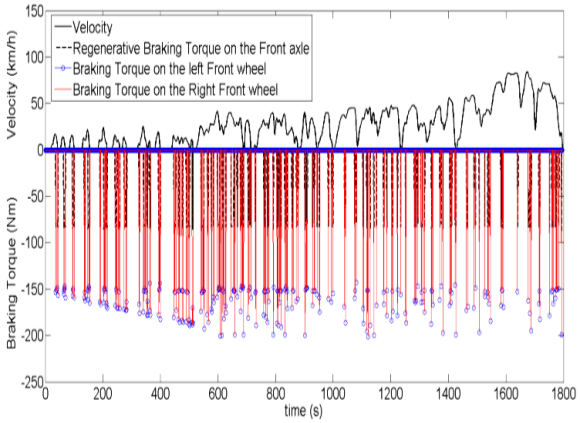


**Figure 14:** Braking torque on the front axle, TEHRAN cycle

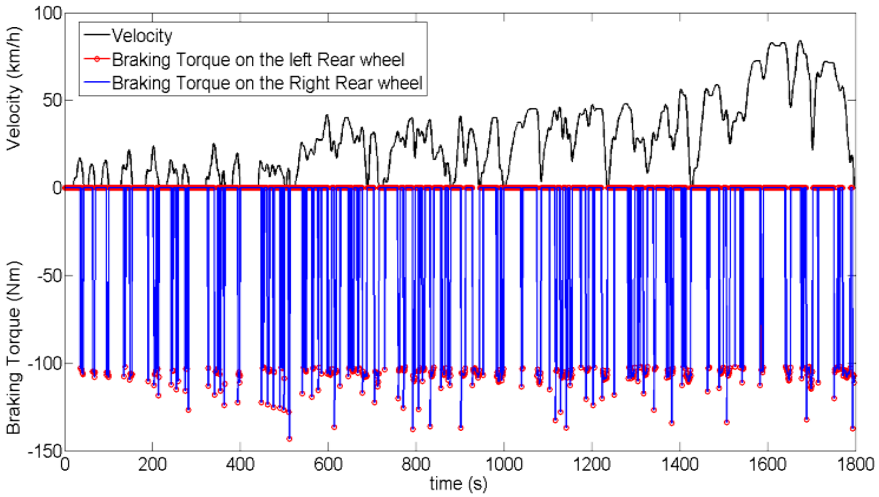


**Figure 15:** Braking torque on the rear axle, TEHRAN cycle

In Table 4 improved parameters of the simulated system has been shown.

Accordance with the result, reduce fuel consumption and energy waste, increase the stored energy and increase the overall efficiency of the system, thus this design is an useful and effective plan.

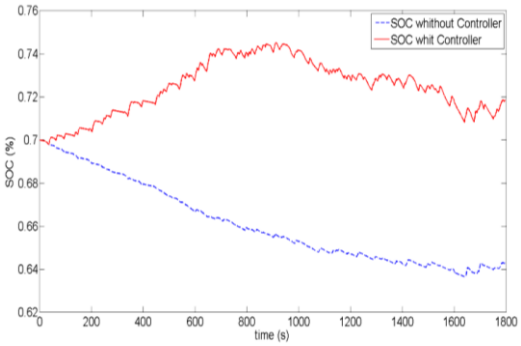


**Figure 16:** Battery SOC, TEHRAN cycle

**Table 4. Simulating result, TEHRAN cycle**

| | With Controller | Without Controller |
|---|---|---|
| Fuel Energy(kJ) | 17059 | 25000 |
| Energy Loss in Motor\Controller (kJ) | 1314\-5844 | 1251\765 |
| SOC in the end of Cycle (%) | 0.7223 | 0.6429 |
| Energy Stored (kJ) | 555 | -1621 |
| overall system Efficiency | 0.099 | 0.061 |

## 3. Conclusions

In this paper, a control system for anti-lock braking control of the hydraulic and regenerative braking system is designed and simulated in ADVISOR. In accordance with the advantages of this design, antilock performance of regenerative braking system, non-interference performance of the regenerative braking system and hydraulic on the front axle, design based on the maximum torque of the electric motor, pay attention to SoC, calculation of the velocity for four wheels separately and possibility of the simulation of the motion in the roads with different slip condition or cornering, are provided.

Simulation results of NEDC cycle shows that with the new controller, fuel consumption has been decreased (13.2%). Also, overall system efficiency has been increased from 9.8% to 11.9%. Reduction of the amount of energy lost and increase of the battery SoC is the other results. The anti-lock and stable performance of the designed system, are shown that this is effective, safe, stable and regenerative.

The controller combines design with anti-slip system during acceleration, hydraulic brake performance in the parking brake and pay attention to the impact and ability to recharge batteries and energy storage are the other proposals in the future.

## Acknowledgements

This research is done in the Road and Railway Vehicle Research Group of the Isfahan University of Technology.

## References

[1] Ehsani M., Gao Y., Cay S., Emadi A., *Modern Electric, Hybrid Electric, and Fuel Cell Vehicle*, CRC Publication, 2005.

[2] J. K. Ahn, K. H. Juog, D. H. Kim, H. B. Jin, H. S. Kim, and S. H. Hwang, "Analysis of a Regenerative Braking System for Hybrid Electric Vehicles Using an Electro-Mechanical Brake," *International Journal of Automotive Technology*, Vol. 10, No. 2, pp. 229−234, 2009.

[3] Xaio Wen-Yong, Wang Feng, and Zhuo Bin, "Regenerative Braking Algorithm for an ISG HEV Based on Regenerative Torque Optimization," *J. Shanghai Jiaotong Univ. (Sci.)*, 13(2): 193–200, 2008.

[4] Ziqiang Chen, Jiaxi Qiang, Jianhui HE, and Lin Yang, "Intelligent Regenerative Braking Control of Hybrid Buses," *Shanghai Jiao Tong University*, 2007.

[5] J. L. Zhang , CH. L. Yin, and J. W. Zhang, "Improvement of Drivablity and Fule Economy with a Hybrid Antiskid Braking System in Hybrid Electric Vehicles," *International Journal of Automotive Technology*, Vol. 11, No. 2, pp. 205−213, 2010.

[6] Tehrani M, Hairi-Yazdi R, Haghpanah-Jahromi B, Esfahanian V, Amiri M, Jafari R. , "Design of an anti-lock regenerative

braking system for a series hybrid electric vehicle". IJAE. 2011; 1 (2):16-20

[7] Ming Lv, Zeyu Chen, Ying Yang, and Jiangman Bi, "Regenerative braking control strategy for a hybrid electric vehicle with rear axle electric drive," 2017 Chinese Automation Congress (CAC), pp. 521–525, .

[8] S. M. Reza Tousi, S. Omid Golpayegani, and Ehsan Sharifian, "Anti-lock regenerative braking torque control strategy for electric vehicle," 2016 IEEE International Conference on Industrial Technology (ICIT), pp. 1418–1423

[9] Majid Ahmadi, Nayereh Raesian, Mahdi Zarif, and Masoud Goharimanesh, "Optimized regenerative brake system using genetic algorithm," 2015 International Congress on Technology, Communication and Knowledge (ICTCK), pp. 177–180, .

[10] Zhongshi Zhang, Junzhi Zhang, Dongsheng Sun, and Chen Lv, "Research on control strategy of electric-hydraulic hybrid anti-lock braking system of an electric passenger car," 2015 IEEE Intelligent Vehicles Symposium (IV), pp. 419–424, .

[11] Hongxiao Yu, Saied Taheri, Jianmin Duan, and Zhiquan Qi, "An Integrated Cooperative Antilock Braking Control of Regenerative and Mechanical System for a Hybrid Electric Vehicle Based on Intelligent Tire," Asian Journal of Control, 2015.

[12] Jian-ping Wen, and Chuan-wei Zhang, "Research on Modeling and Control of Regenerative Braking for Brushless DC Machines Driven Electric Vehicles," Mathematical Problems in Engineering, vol. 2015, pp. 1–6, 2015.

[13] Karami, P., Antilock Regenerative Braking System Design for a Hybrid Electric Vehicle , MSc Thesis, mechanical engineering department, Isfahan University of Technology, 2014.

[14] D. Peng, Y. Zhang, C.-L. Yin, and J.-W. Zhang, "Combined Control of a Regenerative Braking and Anti-lock Braking system for Hybrid Electric Vehicles," *International Journal of Automotive Technology*, Vol. 9, No. 6, pp. 749−757, 2008.

[15] National Renewable Energy Laboratory. Advanced vehicle simulator (ADVISOR). U.S., 2003.

[16] M. Montazeri-Gh, M. Naghizadeh, Development of the Tehran car driving cycle, International Journal of Environment and Pollution, 30 (1) (2007), pp. 106-118